Electronic Supplementary Information

Multifunctional Mixed Valence N-doped CNT@MFe_2O_4 Hybrid Nanomaterials: From Engineered One-Pot Coprecipitation to Application in Energy Storage Paper Supercapacitors

Clara Pereira,*[,a] Rui S. Costa,[a,b] Laury Lopes,[a] Belén Bachiller-Baeza,[c] Inmaculada Rodríguez-Ramos,[c] Antonio Guerrero-Ruiz,[d] Pedro B. Tavares,[e] Cristina Freire,[a] and André M. Pereira*[,b]

[a] REQUIMTE/LAQV, Departamento de Química e Bioquímica, Faculdade de Ciências, Universidade do Porto, Rua do Campo Alegre s/n, 4169-007 Porto, Portugal

[b] IFIMUP and IN – Institute of Nanoscience and Nanotechnology, Departamento de Física e Astronomia, Faculdade de Ciências, Universidade do Porto, 4169-007 Porto, Portugal

[c] Instituto de Catálisis y Petroleoquímica, CSIC, C/ Marie Curie 2, Cantoblanco, 28049 Madrid, Spain

[d] Departamento de Química Inorgánica y Química Técnica, Facultad de Ciencias, UNED, Senda del Rey 9, 28040 Madrid, Spain

[e] Departamento de Química and CQ-VR, Universidade de Trás-os-Montes e Alto Douro, 5001-801 Vila Real, Portugal

***Corresponding authors:**

Dr. Clara Pereira: Tel: +351 220402576; Fax: +351 220402659; e-mail: clara.pereira@fc.up.pt

Prof. André M. Pereira: Tel: +351 220402369; Fax: +351 220402406; e-mail: ampereira@fc.up.pt

Physicochemical characterization (additional information):

TEM: The samples were dispersed in high-purity absolute ethanol under sonication, after which a carbon-coated 400 mesh copper grid was immersed in the suspension and then air-dried.

XPS: A pass energy of 80 eV was used for the survey spectra (step size = 1.0 eV) and 40 eV for the regions of interest (ROI, step size = 0.1 eV). Data acquisition was performed using VISION software at a pressure lower than 1×10^{-6} Pa. Electrostatic charging effects were corrected using a charge neutralization system. The surface atomic percentages were calculated from the corresponding peak areas using the sensitivity factors provided by the manufacturer.

Electrical conductivity measurements: In order to study the intrinsic electrical conductivity (σ) of the as-prepared nanomaterials, the samples were pressed into 13 mm diameter pellets using a laboratory hydraulic press (2 ton, 10 sec), without performing any dilution step (*i.e.*, without previous dispersion in a polymeric matrix).

Table S1. Core-level binding energies and areas of the main components for CNT-N based nanomaterials obtained by curve fitting of XPS spectra[a]

Material	C 1s		N 1s		O 1s		Fe 2p$_{3/2}$		Fe 2p$_{1/2}$		Co 2p$_{3/2}$		Co 2p$_{1/2}$	
	BE (eV)[b]	Area (%)[c]	BE (eV)[b]	Area (%)[c]	BE (eV)[b]	Area (%)[c]	BE (eV)[b]	Area (%)[c]	BE (eV)[b]	Area (%)[c]	BE (eV)[b]	Area (%)[c]	BE (eV)[b]	Area (%)[c]
CNT-N	284.6 (0.9)	44.0	398.4 (1.9)	20.3	530.8 (2.3)	43.6	711.6 (4.5)	100.0	n.d.[d]	n.d.[d]	–	–	–	–
	285.1 (1.4)	22.6	400.0 (1.9)	21.9	532.7 (2.3)	51.8								
	286.2 (1.4)	12.1	401.3 (1.9)	43.1	535.6 (2.3)	4.6								
	287.3 (1.4)	5.4	403.7 (1.9)	10.4										
	288.6 (1.4)	2.4	406.5 (1.9)	4.3										
	290.6 (4.8)	13.5												
CNT-N@Co	284.6 (0.8)	41.3	398.3 (1.7)	16.9	530.0 (1.3)	59.1	710.8 (2.9)[e]	37.2	724.1 (2.9)[e]	14.9	780.1 (2.0)[e]	27.0	795.8 (2.0)[e]	13.4
	285.1 (1.3)	23.4	399.7 (1.7)	24.3	531.4 (1.3)	24.6	713.3 (2.9)[f]	14.5	726.6 (2.9)[f]	7.2	781.8 (2.0)[f]	9.2	797.5 (2.0)[f]	4.6
	286.1 (1.3)	12.3	401.3 (1.7)	44.7	532.4 (1.3)	11.6	718.8 (7.1)[g]	17.5	732.1 (7.1)[g]	8.7	786.9 (5.1)[g]	30.6	802.6 (5.1)[g]	15.2
	287.2 (1.3)	5.6	403.5 (1.7)	11.1	533.5 (1.3)	4.7								
	288.5 (1.3)	3.1	406.0 (1.7)	3.0										
	290.6 (4.8)	14.3												
$CoFe_2O_4$	283.7 (1.6)	12.9	400.0 (1.7)	22.3	530.0 (1.3)	57.8	710.8 (2.9)[e]	32.5	724.1 (2.9)[e]	12.9	780.1 (2.1)[e]	24.6	795.8 (2.1)[e]	12.2
	285.4 (1.6)	54.1	403.2 (1.7)	77.7	531.5 (1.3)	29.0	713.3 (2.9)[f]	14.1	726.6 (2.9)[f]	7.0	781.9 (2.1)[f]	7.6	797.6 (2.1)[f]	3.8
	286.9 (1.6)	21.9			532.5 (1.3)	12.6	718.8 (8.1)[g]	22.3	732.1 (8.1)[g]	11.2	786.9 (6.3)[g]	34.5	802.6 (6.3)[g]	17.3
	288.6 (1.6)	11.1			533.7 (1.3)	0.6								

[a] The core-level binding energies and areas of the trace components in the F 1s and Si 2p regions are presented in the Supporting Information.
[b] The values between brackets refer to the FWHM of the bands.
[c] Area of each component relative to the total core-level peak area.
[d] n.d. – not detected.
[e] Metal cations located in octahedral sites.
[f] Metal cations located in tetrahedral sites
[f] Shake-up satellite peak.

Table S2. Core-level binding energies and areas of the components in the F 1s and Si 2p regions for CNT-N based nanomaterials obtained by curve fitting of XPS spectra

Material	**F 1s**		**Si 2p$_{3/2}$**		**Si 2p$_{1/2}$**	
	BE (eV)[a]	**Area (%)[b]**	**BE (eV)[a]**	**Area (%)[b]**	**BE (eV)[a]**	**Area (%)[b]**
CNT-N	685.7 (4.2)	100	102.4 (2.0)	66.7	103.0 (2.0)	33.3
CNT-N@Co	684.4 (2.0)	100	101.6 (3.0)	66.7	102.2 (3.0)	33.3

[a] The values between brackets refer to the FWHM of the bands.
[b] Area of each component relative to the total core-level peak area.

Table S3. Comparison of the energy storage performance of the paper SCs prepared in this work with that of other paper-based SCs recently reported in the literature[a]

Substrate	Electrode Materials	Electrolyte	Fabrication process	Specific capacitance of the SC cell	Energy density	Power density	Ref.
Nylon filter paper	CNT-N//CNT-N	PVA/H_3PO_4	Vacuum filtration	21.58 F cm^{-3} at 0.5 mV s^{-1} 110.36 mF cm^{-2}	1.44 mW h cm^{-3} 7.37 μW h cm^{-2}	39.53 mW cm^{-3} 202.16 μW cm^{-2}	This work
	CNT-N//CNT-N@Co	PVA/H_3PO_4	Vacuum filtration	14.73 F cm^{-3} at 0.5 mV s^{-1} 53.30 mF cm^{-2}	4.05 mW h cm^{-3} 14.65 μW h cm^{-2}	170.44 mW cm^{-3} 616.73 μW cm^{-2}	
	CNT-N//CNT-N@Mn	PVA/H_3PO_4	Vacuum filtration	25.69 F cm^{-3} at 0.5 mV s^{-1} 123.59 mF cm^{-2}	4.04 mW h cm^{-3} 19.45 μW h cm^{-2}	44.42 mW cm^{-3} 213.73 μW cm^{-2}	
	CNT-N//CNT-N@Fe	PVA/H_3PO_4	Vacuum filtration	20.45 F cm^{-3} at 0.5 mV s^{-1} 89.44 mF cm^{-2}	7.85 mW h cm^{-3} 34.31 μW h cm^{-2}	84.17 mW cm^{-3} 368.09 μW cm^{-2}	
	+CNT-N@Fe//CNT-N@Mn–	PVA/H_3PO_4	Vacuum filtration	22.91 F cm^{-3} at 0.5 mV s^{-1} 95.06 mF cm^{-2}	8.63 mW h cm^{-3} 35.81 μW h cm^{-2}	55.68 mW cm^{-3} 230.99 μW cm^{-2}	
	+CNT-N@Mn//CNT-N@Fe–	PVA/H_3PO_4	Vacuum filtration	21.32 F cm^{-3} at 0.5 mV s^{-1} 88.46 mF cm^{-2}	6.20 mW h cm^{-3} 25.71 μW h cm^{-2}	42.96 mW cm^{-3} 178.19 μW cm^{-2}	
Cellulose filter paper	graphene nanosheets ink	PVA/H_2SO_4	Vacuum filtration	46 mF cm^{-2} (laminated, one cell) 17 mF cm^{-2} (laminated, 3 in-series units)	– 15 μW h cm^{-2} (3 in-series units)	– <100 μW cm^{-2} (3 in-series units)	[1]
Air-laid paper (composed of cellulose and polyester fibers)	CNT ink	KOH	Dip-and-dry process	35 mF cm^{-2} at 1 mA cm^{-2}	–	–	[2]
	CNT ink/MnO_2	KOH		123 mF cm^{-2} at 1 mA cm^{-2}	4.2 μW h cm^{-2}	4000 μW cm^{-2}	
	CNT ink/MnO_2	PVA/KOH		73 mF cm^{-2} at 0.6 mA cm^{-2}	1.8 μW h cm^{-2}	~127 μW cm^{-2} [b]	
Commercial cellulose paper	+$Ni(OH)_2$/Ni/graphite// Mn_3O_4/Ni/graphite–	PVA/NaOH	Spray + pencil drawing + electrodeposition	3.05 F cm^{-3} at 10 mV s^{-1}	0.35 mW h cm^{-3}	32.5 mW cm^{-3}	[3]
Laboratory filter paper	+MnO_2/Ni//AC/Ni–	PVA/Na_2SO_4	electroless plating method electrodeposition	2.0 F cm^{-3} at 5 mV s^{-1} 700 mF cm^{-2}	0.78 mW h cm^{-3}	2.5 mW cm^{-3}	[4]
Lab-made bacterial cellulose paper	Graphene/PANI	H_2SO_4	Vacuum filtration	1320 mF cm^{-2} at 0.25 mA cm^{-2}	120 μW h cm^{-2} 18 μW h cm^{-2}	100 μW cm^{-2} 4450 μW cm^{-2}	[5]

[a] AC – activated carbon; NWs – nanowires; PANI – polyaniline; PPy – polypyrrole. [b] Estimated by eye.

Table S3 (cont.). Comparison of the energy storage performance of the paper SCs prepared in this work with that of other paper-based SCs recently reported in the literature[a]

Substrate	Electrode Materials	Electrolyte	Fabrication process	Specific capacitance of the SC cell	Energy density	Power density	Ref.
Xerox paper	Graphite pencil	H_2SO_4	Pencil drawing	1.13 mF cm^{-2} at 200 mA g^{-1}			[6]
In-house paper	Graphite pencil	H_2SO_4	Pencil drawing	2.3 mF cm^{-2} at 200 mA g^{-1}			[6]
Xerox paper	Thin graphite sheets (pencil)/PPy	PVA/H_3PO_4	Pencil drawing + electrodeposition	52.9 F cm^{-3} at 1 mV s^{-1}			[7]
A4 Xerox paper	Exfoliated graphene ink	PVA/H_2SO_4	Paintbrush coating	~11.3 mF cm^{-2} at 1 mV s^{-1}			[8]
Cellulose nanofiber paper	Positively-charged PANI NWs followed by negatively-charged reduced graphene oxide nanosheets	PVA/H_2SO_4	Dip-coating, layer-by-layer	5.72 mF cm^{-2} at 2 mV s^{-1}			[9]

[a] AC – activated carbon; NWs – nanowires; PANI – polyaniline; PPy – polypyrrole. [b] Estimated by eye.

Fig. S1. Electrical conductivity as a function of the frequency of the CNT-N based nanomaterials in the frequency range of 20 Hz to 3 MHz.

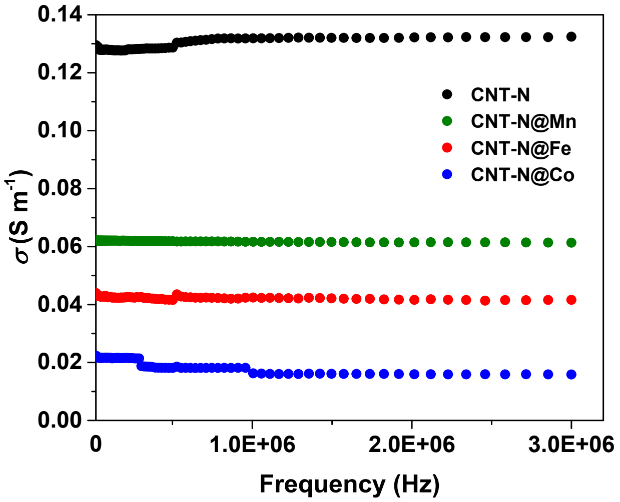

Fig. S2. Cyclic voltammograms of CNT-N//CNT-N paper SC at different scan rates.

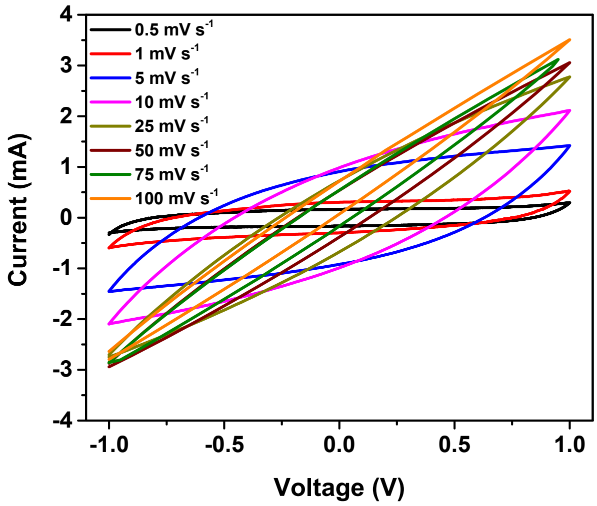

References

1 Z. Weng, Y. Su, D.-W. Wang, F. Li, J. Du and H.-M. Cheng, *Adv. Energy Mater.*, 2011, **1**, 917–922.

2 L. Dong, C. Xu, Y. Li, Z. Pan, G. Liang, E. Zhou, F. Kang and Q.-H. Yang, *Adv. Mater.*, 2016, **28**, 9313–9319.

3 J.-X. Feng, S.-H. Ye, X.-F. Lu, Y.-X. Tong and G.-R. Li, *ACS Appl. Mater. Interf.*, 2015, **7**, 11444–11451.

4 L. Zhang, P. Zhu, F. Zhou, W. Zeng, H. Su, G. Li, J. Gao, R. Sun and C.-P. Wong, *ACS Nano*, 2016, **10**, 1273−1282.

5 R. Liu, L. Ma, S. Huang, J. Mei, J. Xu and G. Yuan, *New J. Chem.*, 2017, **41**, 857–864.

6 G. Zheng, L. Hu, H. Wu, X. Xie and Y. Cui, *Energy Environ. Sci.*, 2011, **4**, 3368–3373.

7 J. Tao, W. Ma, N. Liu, X. Ren, Y. Shi, J. Su and Y. Gao, *Nano-Micro Lett.*, 2015, **7**, 276–281.

8 K. Parvez, Z.-S. Wu, R. Li, X. Liu, R. Graf, X. Feng and K. Müllen, *J. Am. Chem. Soc.*, 2014, **136**, 6083−6091.

9 X. Wang, K. Gao, Z. Shao, X. Peng, X. Wu and F. Wang, *J. Power Sources*, 2014, **249**, 148–155.